

## **SUPPLEMENTARY INFORMATION**

### **Recognisable cerebellar dysplasia associated with mutations in multiple tubulin genes**

R. Oegema<sup>1\*</sup>, T.D. Cushion<sup>2\*</sup>, I.G. Phelps<sup>3</sup>, S-K. Chung<sup>2,4</sup>, J.C. Dempsey<sup>3</sup>, S. Collins<sup>5</sup>, J.G.L. Mullins<sup>2</sup>, T. Dudding<sup>6,7</sup>, H. Gill<sup>8</sup>, A.J. Green<sup>8,9</sup>, W.B. Dobyns<sup>5,10</sup>, G. Ishak<sup>11</sup>, M.I. Rees<sup>2,4†</sup>, D. Doherty<sup>3,5†</sup>

1. Department of Clinical Genetics, Erasmus MC University Medical Centre, Rotterdam, the Netherlands
2. Institute of Life Science, College of Medicine, Swansea University, Swansea SA2 8PP, UK
3. Department of Pediatrics University of Washington, Seattle, WA, USA
4. Wales Epilepsy Research Network (WERN), College of Medicine, Swansea University, Swansea SA2 8PP, UK
5. Center for Integrative Brain Research, Seattle Children's Research Institute, Seattle, WA 98101, USA
6. Hunter Genetics, Waratah, NSW, Australia
7. University of Newcastle, Callaghan, NSW, Australia
8. National Centre for Medical Genetics, Our Lady's Children's Hospital, Dublin 12, Ireland
9. School of Medicine and Medical Science, University College Dublin, Dublin 4, Ireland
10. Departments of Pediatrics and Neurology, University of Washington, Seattle, WA 98195, USA
11. Department of Radiology, Seattle Children's Hospital and University of Washington, Seattle WA 98195, USA

**Supplementary Figure 1. Tubulinopathy-related dysgyria and “diagonal” folia.** A. Example of asymmetrical abnormal shape and orientation of peri-Sylvian gyri without polymicrogyria in UW165-3 with *de novo* *TUBB3* c.1070C>T, p.P357L mutation (brackets) compared to normal control (A') These types of gyral abnormalities can be present anywhere in the cortex. B-D. Relatively normal appearing cerebellum with mild vermis hypoplasia and asymmetric brainstem in UW165-3 compared to normal control (B'-D'). E-H. Characteristic “diagonal” folial pattern (arrowheads) in UW165-3 (B-H) compared to normal control (E'-H'). All images are axial T2-weighted.

**Supplementary Figure 2. Brain imaging of mutation-negative patients:** Representative images from brain MRI, each row represents one patient. DNA was not available for UW161-3. First – third column axial T2 images, fourth column sagittal midline T1 images. The observed abnormalities are similar to the mutation-positive patients (Figure 1). First column, level of the cerebellum and brainstem; brainstem asymmetry and enlarged 4<sup>th</sup> ventricle (black asterisks), normal sized cerebellum (except UW166-3). Second column, level of superior cerebellum showing distinct “diagonal” dysplasia of the foliar pattern. Third column, level of basal ganglia; dysplastic and amorphous basal ganglia in all, also note the irregularities in sulcal depth. Fourth column; thinning of brainstem in all, thin CC in 161-3, UW166-3 and UW146-3. See Table 2 for details of imaging by individual.

**Supplementary Figure 3. Diffusion Tensor Imaging (DTI).** A, B: Axial color-coded fractional anisotropy map at the level of the pons of normal control (A) for comparison and individual UW165-3 (B). Ventral upper (red) tracts: decussation of middle cerebellar peduncles (MCP);

second (blue) tracts: corticospinal tracts (CST); third (red) tracts: transverse pontine fibres; fourth (blue) tracts: dorsal longitudinal pathways. B: attenuation of the transverse pontine and decussating fibres and asymmetry of the right and left pons with suggestion of asymmetry in the CST. C: corresponding axial T2 MR image of the same individual. D, E: fibre tractography of normal control (D) and individual UW165-3 (E). E: asymmetry of the CST in the supratentorium including progressively smaller tract size (black arrow) and misorientated fibres (red arrow) compared to normal. In addition, note that the fibres bundles are less compact compared to normal. Color key: Blue indicates fibre tracks oriented in and out of the plane of the image; red indicates tracks oriented side to side; and green indicates tracks oriented top to bottom.

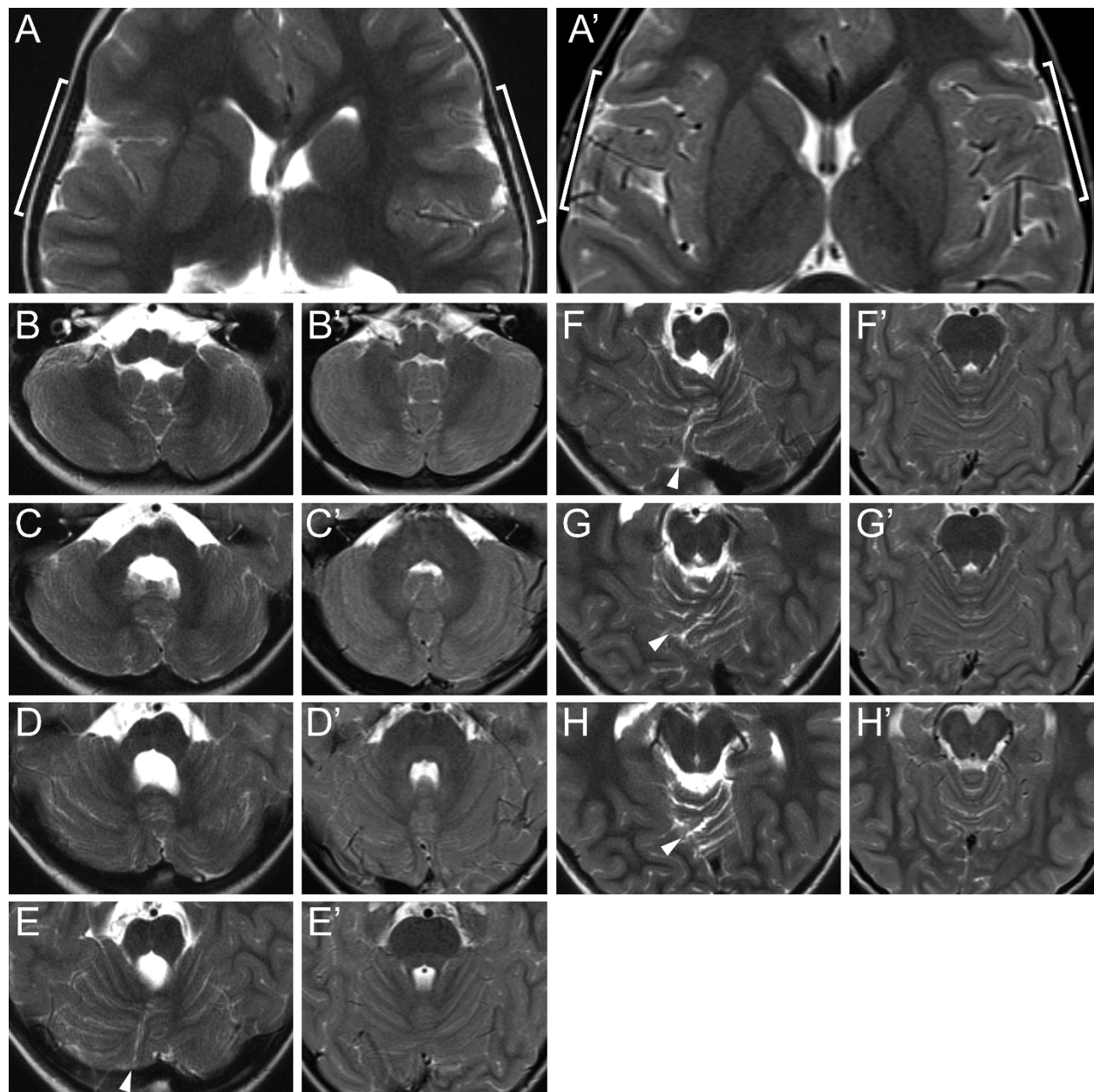
**Supplementary Figure 4. Sanger chromatograms of family UW-169.** Sanger sequencing results show the heterozygous *TUBB2B* c.38G>C mutation in both affected siblings and the mosaic mutation in the father. All DNA derived from leucocytes, except UW169-1 and UW169-5 DNAs derived from saliva.

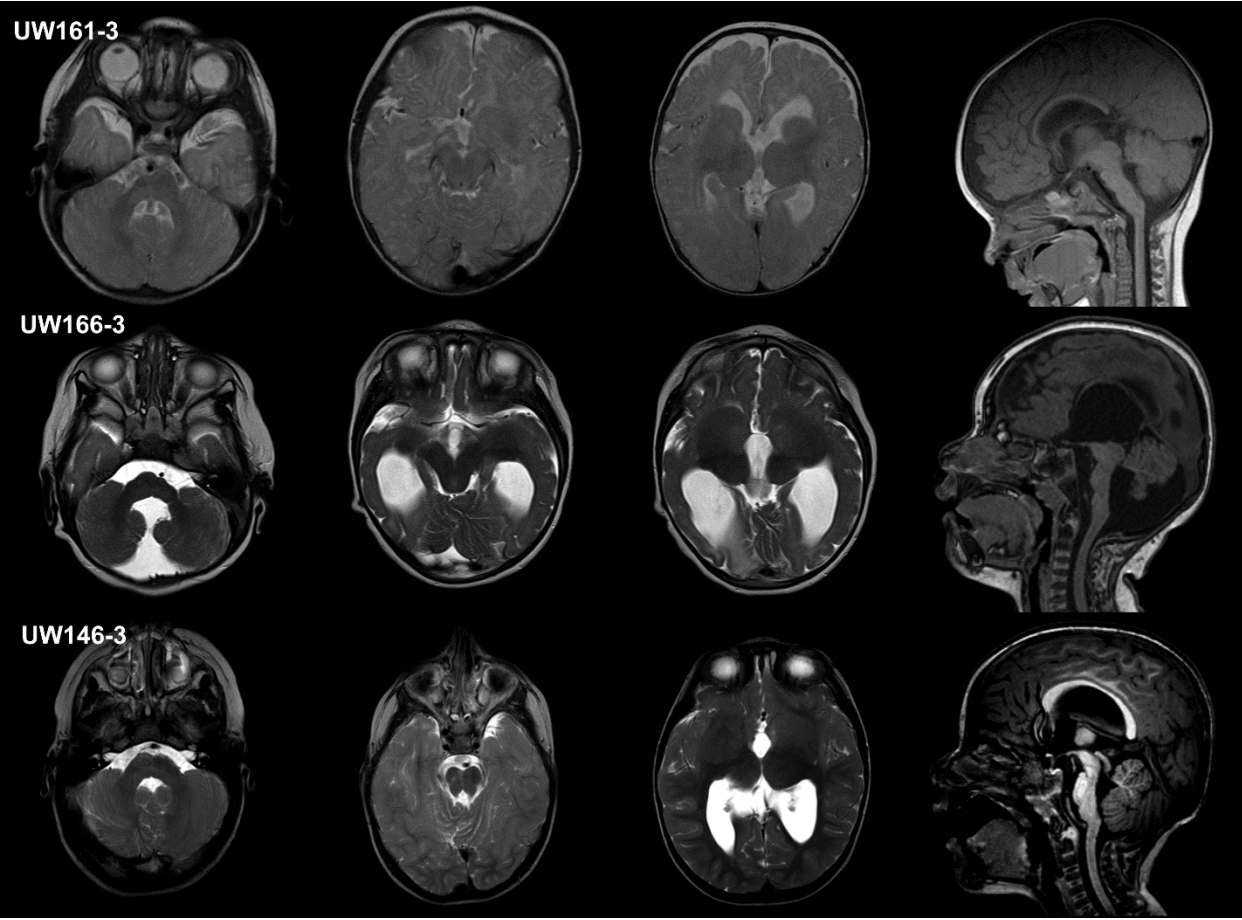
**Supplementary Figure 5. Phylogenetic alignments of tubulin gene variants.** Phylogenetic alignments for (A) TUBA1A p.R214H & p.I219V, (B) TUBB2B p.G13A, (C) TUBB3 p. E288K and (D) TUBB3 p.P357L were created using Clustal Omega (<http://www.ebi.ac.uk/Tools/msa/clustalo/>). Mutant tubulin amino acid sequences are aligned against corresponding wild-type sequences, highly homologous tubulin isotypes in the human genome, and also against equivalent tubulin homologues in other phylogenetic species. Substituted amino acids are highlighted in red with corresponding wild-type residues in bold. Asterisks represent positions with fully conserved residues, colons indicate highly conservative variations, and full stops indicate amino acids with weakly similar properties.

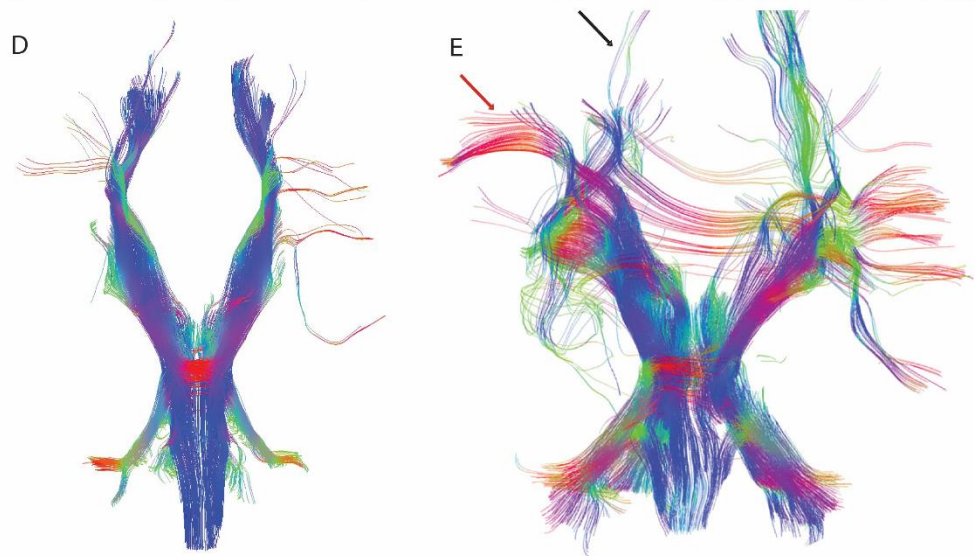
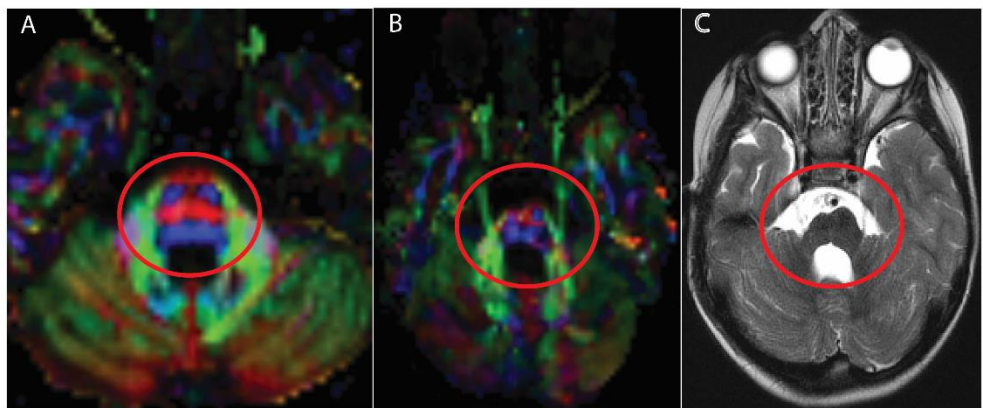
**Supplementary Figure 6. Predicted conformational consequences of the p.G13A substitution on the TUBB2B subunit.** The  $\beta$ G13 residue is positioned within a tight fold between the alpha-helix in which it is located, and the final residues of the preceding beta-strand. This region forms part of the GTP/GDP-binding site of beta-tubulin. The conformation of this fold is facilitated by glycine's lack of side chain (A), whereas substitution with an alanine at this position would introduce an R-group into this region (B). (C) The p.G13A substitution is predicted to subtly alter the conformation of this fold and, as a result, three predicted hydrogen bonds (depicted in green) are lost between the GDP and two polar residues that interact with the nucleotide in this position:  $\beta$ C12 (2 bonds) and  $\beta$ Q11 (Side chains in grey and red show their orientations in the wild-type and variant model, respectively).

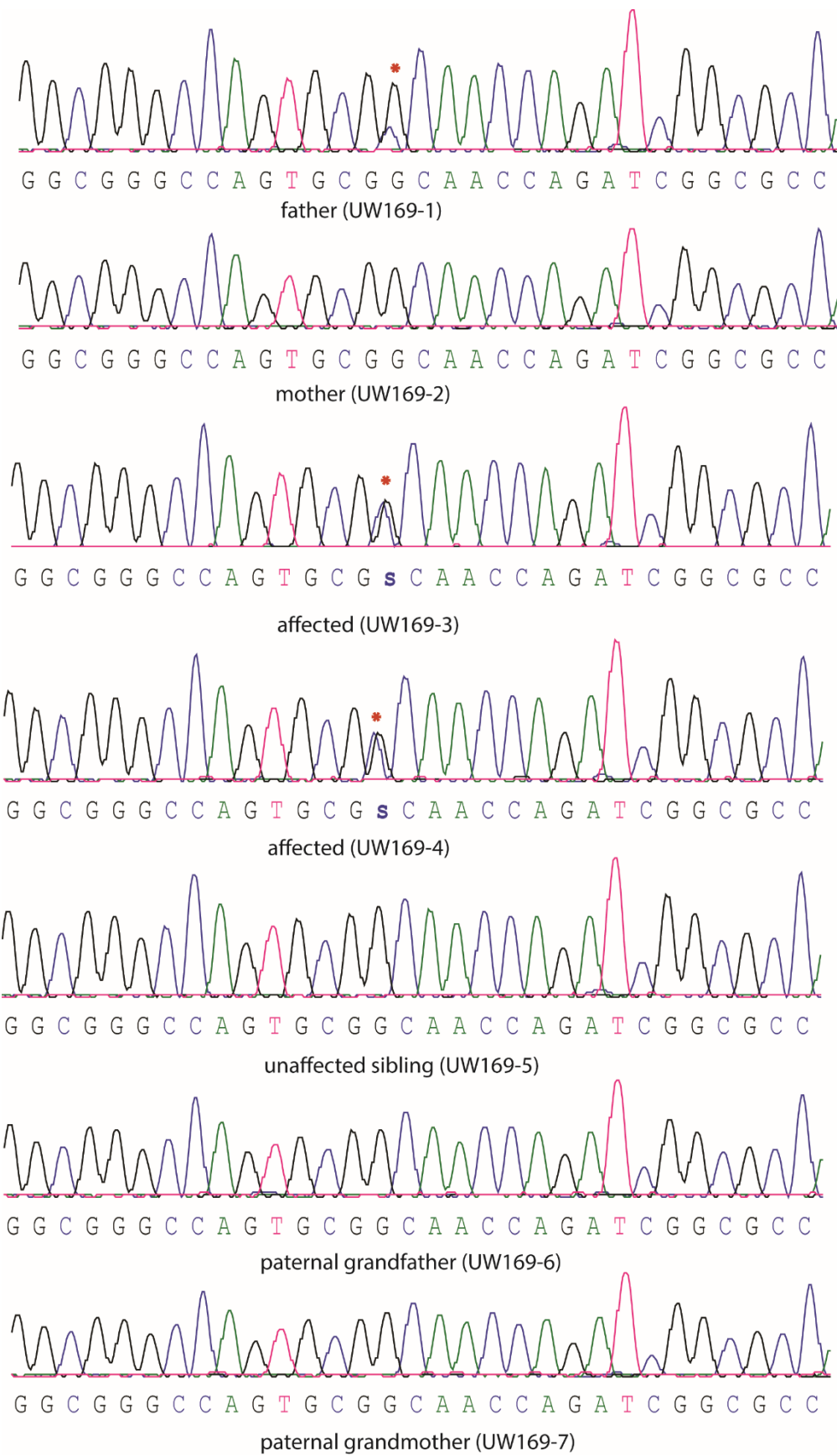
**Supplementary Figure 7. TUBB3 p.E288K is predicted to interrupt two hydrogen bonds.** Two hydrogen bonds (green) between TUBB3 E288 and T285 (grey) are lost by the introduction of lysine (red) at position 288.

**Supplementary Table 1. CADD scores for tubulin gene variants associated with specific cerebral cortical phenotypes.** CADD scores for mutations in *TUBA1A*, *TUBB2B* and *TUBB3* identified in this study as well those published previously (Bahi-Buisson *et al.*, 2014) were generated in order to compare predicted pathogenicities between varying brain abnormalities. Variants are categorised into six phenotypic groups based on those proposed by Bahi-Buisson *et al.*, (2014): microlissencephaly, lissencephaly, central pachygryria, central polymicrogyria-like malformations (PMG), PMG, and simplified gyration.









### A. TUBA1A p.R214H & p.I219V

		*****: * : * . ****	
TUBA1A p.R214H	204	VDNEAIYDIC <b>H</b> RNL <b>D</b> I <b>E</b> RPTYTNLNR	229
TUBA1A p.I219V	204	VDNEAIYDIC <b>R</b> RNL <b>D</b> <b>V</b> ERPTYTNLNR	229
TUBA1A	204	VDNEAIYDIC <b>R</b> RNL <b>D</b> I <b>E</b> RPTYTNLNR	229
TUBA1B	204	VDNEAIYDIC <b>R</b> RNL <b>D</b> I <b>E</b> RPTYTNLNR	229
TUBA1C	204	VDNEAIYDIC <b>R</b> RNL <b>D</b> I <b>E</b> RPTYTNLNR	229
TUBA4A	204	VDNEAIYDIC <b>R</b> RNL <b>D</b> I <b>E</b> RPTYTNLNR	229
TUBA3C	204	VDNEAIYDIC <b>R</b> RNL <b>D</b> I <b>E</b> RPTYTNLNR	229
TUBA3D	204	VDNEAIYDIC <b>R</b> RNL <b>D</b> I <b>E</b> RPTYTNLNR	229
TUBA3E	204	VDNEAIYDIC <b>R</b> RNL <b>D</b> I <b>E</b> RPTYTNLNR	229
TUBA8	204	VDNEAIYDIC <b>R</b> RNL <b>D</b> I <b>E</b> RPTYTNLNR	229
<i>P.troglodytes</i>	204	VDNEAIYDIC <b>R</b> RNL <b>D</b> I <b>E</b> RPTYTNLNR	229
<i>M.mulatta</i>	146	VDNEAIYDIC <b>R</b> RNL <b>D</b> I <b>E</b> RPTYTNLNR	194
<i>C.lupus</i>	204	VDNEAIYDIC <b>R</b> RNL <b>D</b> I <b>E</b> RPTYTNLNR	229
<i>B.taurus</i>	204	VDNEAIYDIC <b>R</b> RNL <b>D</b> I <b>E</b> RPTYTNLNR	229
<i>M.musculus</i>	204	VDNEAIYDIC <b>R</b> RNL <b>D</b> I <b>E</b> RPTYTNLNR	229
<i>R.norvegicus</i>	204	VDNEAIYDIC <b>R</b> RNL <b>D</b> I <b>E</b> RPTYTNLNR	229
<i>G.gallus</i>	146	VDNEAIYDIC <b>R</b> RNL <b>D</b> I <b>E</b> RPTYTNLNR	194
<i>D.rerio</i>	204	VDNEAIYDIC <b>R</b> RNL <b>D</b> I <b>E</b> RPTYTNLNR	229
<i>X.tropicalis</i>	204	VDNEAIYDIC <b>R</b> RNL <b>D</b> I <b>E</b> RPTYTNLNR	229
<i>C.elegans</i>	204	<b>M</b> DNEAIYE <b>I</b> TKVN <b>L</b> GVRSPTYTHLN <b>R</b>	229

### B. TUBB2B p.G13A

		****: * : * *****: :	
TUBB2B p.G13A	1	MREIVHIQAGQC <b>A</b> NQIGAKFWEVIS	25
TUBB2B	1	MREIVHIQAGQC <b>G</b> NQIGAKFWEVIS	25
TUBB3	1	MREIVHIQAGQC <b>G</b> NQIGAKFWEVIS	25
TUBB	1	MREIVHIQAGQC <b>G</b> NQIGAKFWEVIS	25
TUBB1	1	MREIVHIQ <b>I</b> GQC <b>G</b> NQIGAKFWEM <b>I</b> G	25
TUBB2A	1	MREIVHIQAGQC <b>G</b> NQIGAKFWEVIS	25
TUBB4B	1	MREIVH <b>I</b> QAGQC <b>G</b> NQIGAKFWEVIS	25
TUBB4A	1	MREIVH <b>I</b> QAGQC <b>G</b> NQIGAKFWEVIS	25
TUBB6	1	MREIVHIQAGQC <b>G</b> NQIG <b>T</b> KFWEVIS	25
<i>P.troglodytes</i>	1	MREIVHIQAGQC <b>G</b> NQIGAKFWEVIS	25
<i>M.mulatta</i>	1	MREIVHIQAGQC <b>G</b> NQIGAKFWEVIS	25
<i>C.lupus</i>	1	MREIVHIQAGQC <b>G</b> NQIGAKFWEVIS	25
<i>B.taurus</i>	1	MREIVHIQAGQC <b>G</b> NQIGAKFWEVIS	25
<i>M.musculus</i>	1	MREIVHIQAGQC <b>G</b> NQIGAKFWEVIS	25
<i>R.norvegicus</i>	1	MREIVHIQAGQC <b>G</b> NQIGAKFWEVIS	25
<i>G.gallus</i>	1	MREIVHIQAGQC <b>G</b> NQIGAKFWEVIS	25
<i>D.rerio</i>	1	MREIVH <b>I</b> QAGQC <b>G</b> NQIGAKFWEVIS	25
<i>D.melanogaster</i>	1	MREIVHIQAGQC <b>G</b> NQIG <b>G</b> KFWEVIS	25
<i>X.tropicalis</i>	1	MREIVHIQAGQC <b>G</b> NQIGAKFWEVIS	25
<i>C.elegans</i>	1	MREIVHIQAGQC <b>G</b> NQIG <b>S</b> KFWEVIS	25
<i>A.thaliana</i>	1	MREILHIQ <b>G</b> QC <b>G</b> NQIGAKFWEV <b>V</b> C	25

### C. TUBB3 p.E288K

		: . * * * : : * * * * : * : * * *	
TUBB3 p.E288K	275	RGSQQYRALTVPKLTQQMFDAKNMM	300
TUBB3	275	RGSQQYRALTVPELTQQMFDAKNMM	300
TUBB2B	275	RGSQQYRALTVPELTQQMFDSKNMM	300
TUBB	275	RGSQQYRALTVPELTQQVFDAKNMM	300
TUBB1	275	QGSQQYRALSVATELTQQMFDAKNMM	300
TUBB2A	275	RGSQQYRALTVPELTQQMFDSKNMM	300
TUBB4B	275	RGSQQYRALTVPELTQQMFDAKNMM	300
TUBB4A	275	RGSQQYRALTVPELTQQMFDAKNMM	300
TUBB6	275	RGSQQYRALTVPELTQQMFDAKNMM	300
<i>P. troglodytes</i>	275	RGSQQYRALTVPELTQQMFDAKNMM	300
<i>M. mulatta</i>	275	RGSQQYRALTVPELTQQMFDSKNMM	300
<i>C. lupus</i>	275	RGSQQYRALTVPELTQQMFDAKNMM	300
<i>B. taurus</i>	275	RGSQQYRALTVPELTQQMFDAKNMM	300
<i>M. musculus</i>	275	RGSQQYRALTVPELTQQMFDAKNMM	300
<i>R. norvegicus</i>	275	RGSQQYRALTVPELTQQMFDAKNMM	300
<i>G. gallus</i>	275	RGSQQYRALTVPELTQQMFDAKNMM	300
<i>D. rerio</i>	275	RGSQQYRSLTVPELTQQMFDAKNMM	300
<i>D. melanogaster</i>	275	RGSQQYRALTVPELTQQMFDAKNMM	300
<i>X. tropicalis</i>	275	RGSQQYRALTVPELTQQMFDAKNMM	300
<i>C. elegans</i>	275	RSNQQYRAITVPELTQQCFDAKNMM	300
<i>A. thaliana</i>	275	RGSQQYRSLTVPELTQQMWD SKNMM	300

### D. TUBB3 p.P357L

		***** * : ***** * *. * : *****	
TUBB3 p.P357L	345	IPNNVKAVCDILPRGLKMSSTFIG	369
TUBB3	345	IPNNVKAVCDIPPRGLKMSSTFIG	369
TUBB2B	345	IPNNVKTAVCDIPPRGLKMSATFIG	369
TUBB	345	IPNNVKTAVCDIPPRGLKMAVTFIG	369
TUBB1	345	IPNNVKAVCDIPPRGLSMAATFIG	369
TUBB2A	345	IPNNVKTAVCDIPPRGLKMSATFIG	369
TUBB4B	345	IPNNVKTAVCDIPPRGLKMSATFIG	369
TUBB4A	345	IPNNVKTAVCDIPPRGLKMAATFIG	369
TUBB6	345	IPNNVKAVCDIPPRGLKMASTFIG	369
<i>P. troglodytes</i>	345	IPNNVKAVCDIPPRGLKMSSTFIG	369
<i>M. mulatta</i>	345	IPNNVKTAVCDIPPRGLKMSATFIG	369
<i>C. lupus</i>	345	IPNNVKAVCDIPPRGLKMSSTFIG	369
<i>B. taurus</i>	345	IPNNVKAVCDIPPRGLKMSSTFIG	369
<i>M. musculus</i>	345	IPNNVKAVCDIPPRGLKMSSTFIG	369
<i>R. norvegicus</i>	345	IPNNVKAVCDIPPRGLKMSSTFIG	369
<i>G. gallus</i>	345	IPNNVKAVCDIPPRGLKMSSTFIG	369
<i>D. rerio</i>	345	IPNNVKTAVCDIPPRGLKMAATFIG	369
<i>D. melanogaster</i>	345	IPNNCKTAVCDIPPRGLKMSATFIG	369
<i>X. tropicalis</i>	345	IPNNVKAVCDIPPRGLKMASTFIG	369
<i>C. elegans</i>	345	IPNNVKTAVCDIPPRGLKMSATFIG	369
<i>A. thaliana</i>	345	IPNNVKSTVCDIPPTGLKMASTFIG	369

